Design for a Self-Packaged All-PCB Wideband Filter with Good Stopband Performance

B. A. Belyaev[#$1], A.M. Serzhantov[$2], Ya. F. Bal'va[#3], and An. A. Leksikov[#4]
[#] Kirensky Institute of Physics SB RAS, Krasnoyarsk, Russia
[$] Siberian Federal University, Krasnoyarsk, Russia
[1]belyaev@iph.krasn.ru, [2]cubicus@mail.ru, [3] ya.f.balva@mail.ru, [4]a.a.leksikov@gmail.com

***Abstract*— A new design of a self-packaged all-PCB ultrawideband filter based on the cascade connection of high-pass and low-pass filters is presented. The novel low-pass and high-pass quasi-lumped filter structure differs from the known one by the existence of cross-coupling between elements producing transmission zeroes at the desired frequency. The filter fabricated using materials with a rather low quality factor has demonstrated a good performance: the central frequency is 0.99 GHz, the 1 dB bandwidth is 151%, the minimum in-band loss is 0.3 dB, the selectivity ($\Delta f_{30dB}/\Delta f_{3dB}$) is 1.21, and the 40 dB stopband width is 6.10f_0.**

***Keywords*— bandpass filter, low-pass filters, wideband filter.**

I. Introduction

The development of modern communication systems requires the design of ultrawideband filters [1-6] due to the need to increase the speed of data transmission through communication channels. The development of ultrawideband bandpass filters, which are the most important devices in communication systems, is a difficult task since simultaneous with the formation of a passband of more than 100%, it is necessary to ensure both high selectivity of the devices and large depth and width of the stopbands. At the same time, filters must be shielded since they are very sensitive to EMC, so they either should be installed in a metallic case, or have a self-packaged design. PCB technology is currently the main technology used to design self-packaged filters [7,8,9], couplers [10], and power dividers [11] have already been presented.

In all-PCB bandpass filters, top and bottom metallic covers are formed by metallic layers on boards, while sidewalls, grounding and board fastening are realized by metallic vias from the top to the bottom substrate. The vias can be metallized either by galvanic growth of copper [4] or by installation of metal bushings [7,8,11] in the holes, without prepreg layers in both cases. However, filters fabricated by the first method are weakly resistant to mechanical vibrations as the boards have point connections; to increase the vibration resistance, one needs to increase the number of vias. The second method is vibration resistant, but it is much more laborious and increases filter production costs.

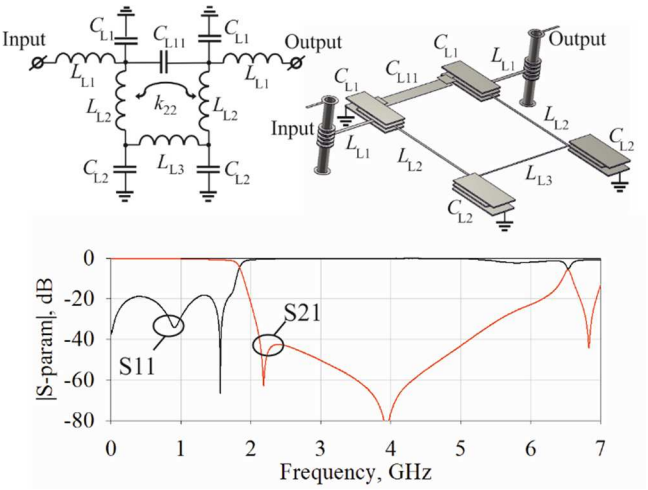

Fig. 1. Low-pass filter design, its equivalent circuit and frequency response of the 3D model for the current configuration.

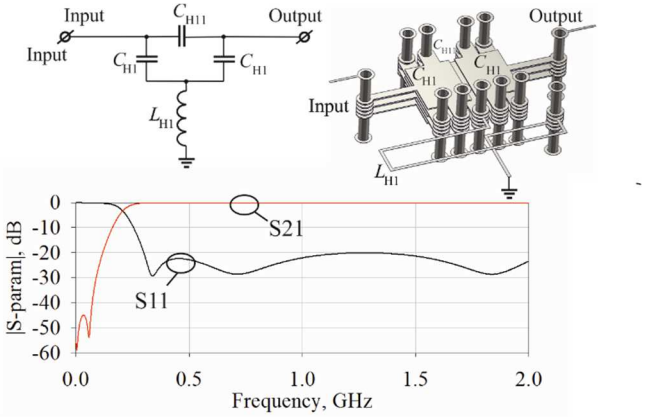

Fig. 2. High-pass filter design, its equivalent circuit and frequency response of the 3D model for the current configuration.

In this paper, we propose a self-packaged all-PCB wideband filter with good performance and low weight. The proposed filter consists of a cascade of multilayer low-pass (LPF) and high-pass (HPF) filters designed for the standard PCB technology where metallized laminates are bonded with prepreg.

2021 IEEE/MTT-S International Microwave Symposium - IMS 2021 | 978-1-6654-0307-8/21/$31.00 ©2021 IEEE | DOI: 10.1109/IMS19712.2021.9575012

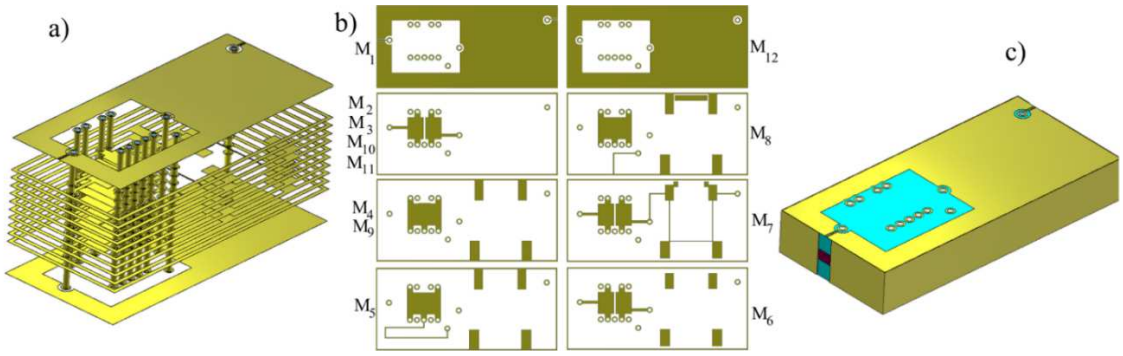

Fig. 3. The filter structure (side walls and substrates are hidden), layers topologies and the structure appearance.

II. LPF STRUCTURE

It is obvious that the selectivity of the filter and the low- and high-frequency stopband performance are determined by the selectivity of the LPF and HPF involved in the filter structure. In this structure, we have used both a new LPF and a new HPF, which are characterized by increased selectivity due to designing the required number of transmission zeros in the frequency response.

The LPF structure is presented in Fig. 1 and consists of inductances and quasi-lumped capacitances (four in the current case) grounded by one plate and connected via an inductance to a 50-Ohm line with a second plate. The difference in the proposed structure from the known ones lies in the cross-coupling between the stubs that produces a zero pole in the frequency response. In the current configuration (equivalent circuit presented in Fig. 1), two additional couplings exist that produce two zero poles in the stopband. Capacitance C_{L11} is responsible for zero pole close to the passband, and can be tuned independently, so one can increases a roll-off of the filter. The mutual coupling between inductances L_2 produces the second zero pole at a higher frequency. The proposed structure is scalable, and the addition of the new elements produces an extra pole in the frequency response. In a similar in-line structure [12], in which elements are arranged alternately on opposite sides of the transmission line, a 5-stub filter will have 5 additional zero poles that significantly increase the slope of the LPF. In the current design, we have used a 4-stub structure with an additional coupling between the 1st and 4th stubs, and a total number of zero poles equal to 2.

III. HPF STRUCTURE.

The model of the HPF structure and its equivalent circuit are presented in Fig. 2. The HPF structure corresponds to a first-order lumped-element filter with one zero pole in the stopband at frequency ω_z, which does not depend on the wave impedance of the input and output ports and is determined by the expression:

$$\omega_z = \omega_0 \cdot K_C, \quad (1)$$

where $\omega_0 = 1/\sqrt{2L_1C_1}$ is the resonant frequency of the circuit with grounded input and output, and

$K_C = \sqrt{2C_{12}/(C_1 + 2C_{12})}$ is a coefficient that reflects the value of the capacitive coupling between the input and the output.

From a practical point of view, it is important that the zero-pole frequency ω_z is proportional to the coefficient K_C, which can be varied over a wide range by varying the gap between capacitor plates. This allows one to obtain deep suppression at the required frequencies in a filter's stopband.

IV. BPF STRUCTURE

The BPF model structure and layer topologies are presented in Fig. 3. A serial connection of the LPF and HPF is used, where the characteristics of the high-frequency slope and stopband are determined by the LPF, while the HPF response determines the low-frequency slope and stopband.

A 6-layer all-PCB structure (Fig. 3a) was used to design and fabricate the BPF. The filter structure, arranged at four RO4003C 0.254-mm substrates, is separated from grounding layers by an F4BM ($\varepsilon = 2.55$, $\tan\delta = 0.0007$) substrate having a 2 mm thickness. The substrates are bonded with RO4450B prepreg ($\varepsilon = 3.3$, $\tan\delta = 0.004$ $h_d = 0.091$ mm). To compensate for the effect of prepreg application for filter fabrication (the prepreg thickness after the bonding process strongly depends on the topology), all the capacitor plates are designed with double metallization mirroring on both sides of the prepreg layer. The total number of metal layers in the structure is 12, as both surfaces of the substrates are involved in the topology. The layers M1 and M12 differ only by tapping lines. The layers M2, M3, M10 and M11 have the same topology consisting of the capacitor plate of the HPF. The layer M6 has the same topology as the HPF but also contains the capacitor plate of the LPF. The layers M4 and M9 are the same, consisting of capacitances of both the LPF and HPF, and the layers M5, M7 and M8 differ from each other and consist of both capacitances and inductances of the LPF and HPF. The HPF and LPF are cascade by 0.2-mm width stripline, which is situated on the layer M7, and connects the inductance L_{L1} of the LPF and capacitance C_{H1} of HPF.

To organize a connection of the topologies of all layers, 13 metallized 0.7-mm vias are fabricated: 11 for the HPF and 2 for shifting feed points to the external layers. The grounding of the internal layers can be done either by designing a framework around the topology to which the grounded conductors are attached (Fig. 3b) or by directly connecting the conductors to the sidewalls of the structure.

One of the main advantages of the structure is that its sidewalls are obtained by the method of galvanic growth of

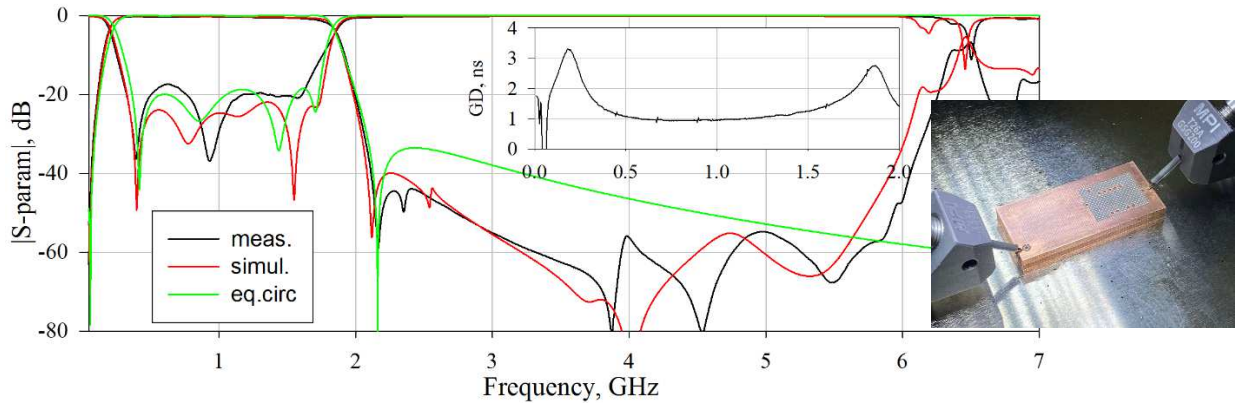

Fig. 4. Frequency response of the designed (red curve), fabricated (black curve) filter and its equivalent circuit (green curve). The group delay and the photograph of the fabricated filter in the inset.

copper (electroplating) common to PCB technology, the same as that used for via metallization. In the current case, the thickness of the side metallization was 20 μm. The only non-metallized windows remaining at the sidewalls of the filter are bridges used for holding filter structures in the common board during the fabrication of the multilayer structure and are milled in the last stage of manufacturing. The window positions are determined by the feedline positions. This solution significantly reduces the weight of the filter and makes it compatible with standard PCB technology.

A 150% filter was designed and fabricated, with 1 dB cut-off frequencies of 0.25 GHz for the HPF and 1.75 GHz for the LPF. During the filter synthesis procedure, the primary parameters of the LPF and HPF were obtained independently. At the same time, the filter was fine-tuned when both structures were present in the topology, since, due to the close arrangement of the filter topologies, their mutual influence on each other is observed. The equivalent circuit parameters are as follows: C_{L1} = 2.7 pF, C_{L2} = 3.3 pF, C_{L11} = 0.075 pF, C_{H1} = 10 pF, C_{H11} = 0.33 pF, L_{L1} = 4 nH, L_{L2} = 8.3 nH, L_{L3} = 8.45 nH, and L_{H1} = 20.9 nH. In Fig. 4, a comparison of the frequency responses of the simulated filter, fabricated filter and its equivalent circuit is presented. All the curves are very similar in the passband; even the frequency responses closest to the passband transmission zeros (insets in Fig. 4) are nearly the same. The only difference lies in the absence of the transmission zero for the equivalent circuit, as the cross-coupling k_{22} was not realized in it.

V. Conclusion

A new design of a self-packaged all-PCB wideband filter based on the cascade connection of high-pass and low-pass filters is presented. The filter differs from the known filters in that it is fully compatible with industrial PCB technology: dielectric layers are bonded with prepreg, sidewalls are obtained by electroplating. The high-pass and low-pass filter designs used in the filter are scalable and allow the filter performance to be significantly increased through transmission zeros in the stopbands. The fabricated filter with a size of 35×16×5.3 mm^3 ($0.12\lambda_0\times0.055\lambda_0\times0.018\lambda_0$) displays the following performance: the central frequency is 0.99 GHz, the 1 dB bandwidth is 151%, the minimum in-band loss is 0.3 dB, the selectivity ($\Delta f_{30dB}/\Delta f_{3dB}$) is 1.21, and the 40 dB stopband width is $6.10f_0$.

Table 1. Performance comparison with other works.

Ref.	Self-package	f_0 (GHz)	FBW (%)	Size (λ_g^2)	IL(dB)	Upper stopband (dB)
[1]	No	1.25	120	0.002	0.7	-10 ($4.0f_0$)
[2]	No	1.2	123	0.024	0.3	-30 ($4.5f_0$)
[3]	No	5.5	101.8	0.052	1.2	-20 ($3.1f_0$)
[4]	Yes	6.85	118	0.26	1.1	-17($2.5f_0$)
[5]	No	6.48	111	0.041	2.2	-10 ($4.6f_0$)
[6]	No	7.3	115	0.003	1.5	-15 ($2.7f_0$)
[7]	Yes	5.48	14.8	0.303	1.44	-40 ($1.6f_0$)
This work	Yes	0.99	151	0.007	1.0	-40 ($6.16f_0$)

References

[1] D. Ding, Q. Zhang, J. Xia, A. Zhou and L. Yang, "Wiggly Parallel-Coupled Line Design by Using Multiobjective Evolutionay Algorithm," IEEE Microwave and Wireless Components Letters, vol. 28, no. 8, pp. 648-650, Aug. 2018.

[2] X. Gao, W. Feng and W. Che, "Compact Ultra-Wideband Bandpass Filter With Improved Upper Stopband Using Open/Shorted Stubs," IEEE Microwave and Wireless Components Letters, vol. 27, no. 2, pp. 123-125, Feb. 2017.

[3] M. M. Honari, R. Mirzavand, H. Saghlatoon and P. Mousavi, "Two-Layered Substrate Integrated Waveguide Filter for UWB Applications," IEEE Microwave and Wireless Components Letters, vol. 27, no. 7, pp. 633-635, July 2017.

[4] S. Qian and J. Hong, "Miniature Quasi-Lumped-Element Wideband Bandpass Filter at 0.5–2-GHz Band Using Multilayer Liquid Crystal Polymer Technology," IEEE Transactions on Microwave Theory and Techniques, vol. 60, no. 9, pp. 2799-2807, Sept. 2012.

[5] C.-H. Wu, Y.-S. Lin, C.-H. Wang and C. H. Chen, "A compact LTCC ultra-wideband bandpass filter using semi-lumped parallel-resonance circuits for spurious suppression," in 2007 European Microwave Conference, Munich, 2007, pp. 532-535

[6] Y. Dai, Q. Han, Q. Xie, F. Guo, L. Wang and C. Wei, "A novel compact LTCC UWB bandpass filter using semi-lumped highpass filter," in 2012 Asia Pacific Microwave Conference Proceedings, Kaohsiung, 2012, pp. 502-504

[7] C. Du, K. Ma, T. Feng and S. Mou, "A self-packaged bandpass filter with controllable transmission zeros using Substrate Integrated Suspended Lines," in 2016 IEEE International Conference on

Microwave and Millimeter Wave Technology (ICMMT), Beijing, 2016, pp. 317-319.
[8] Y. Chu, K. Ma, Y. Wang and F. Meng, "A Self-Packaged Low-Loss and Compact SISL DBBPF With Multiple TZs," IEEE Microwave and Wireless Components Letters, vol. 29, no. 3, pp. 192-194, March 2019.
[9] H. Zha, F. Kong and Z. Hao, "A miniature bandpass filter using multilayered PCB technology,"in 2017 Sixth Asia-Pacific Conference on Antennas and Propagation (APCAP), Xi'an, 2017, pp. 1-3.
[10] Y. Wang, K. Ma and S. Mou, "A compact self-packaged lumped-element coupler using substrate integrated suspended line technology," in 2016 IEEE MTT-S International Microwave Symposium (IMS), San Francisco, CA, 2016, pp. 1-3.
[11] Feng, K. Ma and Y. Wang, "A Self-Packaged SISL Dual-Band Power Divider for WLAN Application with Low Loss and Compact Size," in 2019 IEEE MTT-S International Microwave Symposium (IMS), Boston, MA, USA, 2019, pp. 436-439.
[12] B.A Belyaev, A.M. Serzhantov, A.A. Leksikov, et al. “A Highly Selective Stripline Lowpass Filter with More Than 100-dB Wide Stopband Attenuation” in Tech. Phys. Lett. Vol. 46, pp. 364–367, 2020